Thieme

Ultra-short echo time (UTE) MR imaging: A brief review on technical considerations and clinical applications

MR-Bildgebung mit ultrakurzen Echozeiten: ein kurzer Überblick zu methodischen Überlegungen und klinischen Anwendungen

Authors

Anne Slawig[1, 2] , Maik Rothe[1, 2], Andreas Deistung[1, 2], Klaus Bohndorf[1], Richard Brill[1], Simon Graf[1, 2], Andreas Max Weng[3], Walter A Wohlgemuth[1, 2], Alexander Gussew[1, 2]

Affiliations

1 University Clinic and Outpatient Clinic for Radiology, University Hospital Halle, Germany
2 Halle MR Imaging Core Facility, Medical faculty, Martin Luther University Halle Wittenberg, Halle, Germany
3 Department of Diagnostic and Interventional Radiology, University Hospital Wurzburg, Wurzburg, Germany

Correspondence

Anne Slawig
University Clinic and Outpatient Clinic for Radiology, University Hospital Halle, Ernst-Grube Str. 40, 06120 Halle, Germany
anne.slawig@uk-halle.de

ABSTRACT

Background With the availability of MRI sequences with ultrashort echo times (UTE sequences), a signal can be gained from tissue, which was formerly only indirectly accessible. While already extensively employed in various research settings, the widespread transition of UTE imaging to clinical practice is just starting.

Methods Based on a systematic literature search as well as knowledge gained through annual participation in conferences dedicated to advances in MRI, this review aims to give a brief overview of technical considerations and challenges of UTE imaging and summarizes the major areas of application of UTE imaging.

Results UTE is already employed in clinical practice for structural lung imaging as well as the characterization of tissue composition and its alterations in selected musculoskeletal, cardiovascular, or neurodegenerative diseases. In specific contexts it can replace CT examinations with ionizing radiation and is especially attractive for pediatric patients and longitudinal monitoring of disease progression and treatment.

Conclusion UTE imaging provides an interesting and very valuable tool for various clinical purposes and promises a multitude of new insights into tissue properties. While some challenges remain, ongoing adoption in the clinical routine can be expected, as UTE approaches provide a new contrast and capture a signal in tissue formerly invisible on MR imaging.

Key Points
- UTE imaging gains relevance in clinical settings
- UTE imaging is employed for the characterization of tissue composition and its alterations in selected musculoskeletal, cardiovascular, or neurodegenerative diseases
- UTE imaging is employed in the clinical routine for structural lung imaging
- UTE imaging promises a multitude of new insights into tissue properties

ZUSAMMENFASSUNG

Hintergrund Mit der Verfügbarkeit von MRT-Sequenzen mit Ultrakurzzeit-Echos (UTE-Sequenzen) wird die direkte Bildgebung von Gewebeanteilen möglich, die bisher nur indirekt als dunkle Region im Kontrast zu hellen Strukturen zugänglich waren. Während die UTE-Bildgebung in der Forschung bereits in großem Umfang eingesetzt wird, steht der Übergang in die klinische Praxis noch am Anfang.

Methoden Basierend auf einer systematischen Literaturrecherche sowie Erkenntnissen, die durch die jährliche Teilnahme an Konferenzen zu Fortschritten in der MRT gewonnen wurden, soll dieses Review einen kurzen Überblick über die

technischen Überlegungen und Herausforderungen der UTE-Bildgebung geben und die wichtigsten Anwendungsbereiche zusammenfassen, in denen diese bereits Einzug gehalten hat.
Ergebnisse UTE-Bildgebung wird bereits in der Klinik zur strukturellen Lungenbildgebung sowie zur Charakterisierung der Gewebezusammensetzung und ihrer Veränderungen bei ausgewählten Erkrankungen des Bewegungsapparats, des Herz-Kreislauf-Systems oder bei neurodegenerativen Erkrankungen eingesetzt. Unter bestimmten Rahmenbedingungen kann es strahlungsintensive CT-Untersuchungen ersetzen und ist besonders attraktiv für pädiatrische Patienten und die Langzeitüberwachung von Krankheitsverläufen und Behandlungen.
Schlussfolgerung Die UTE-Bildgebung ist ein vielversprechendes Verfahren für verschiedene klinische Zwecke und verspricht eine Vielzahl neuer Erkenntnisse zu Gewebeeigenschaften. Auch wenn noch einige Herausforderungen zu bewältigen sind, ist eine fortschreitende Etablierung der UTE-Bildgebung in der klinischen Routine abzusehen, da sie einen neuen Bildkontrast bietet und Signale im Gewebe erfassen kann, die der MR-Bildgebung bisher verschlossen geblieben sind.

Kernaussagen

- UTE-Bildgebung gewinnt an Relevanz im klinischen Umfeld.
- UTE-Bildgebung wird zur Charakterisierung der Gewebezusammensetzung und deren Veränderungen bei ausgewählten muskuloskelettalen, kardiovaskulären oder neurodegenerativen Erkrankungen eingesetzt.
- UTE-Bildgebung wird in der Klinik zur strukturellen Lungenbildgebung eingesetzt.
- UTE-Bildgebung verspricht eine Vielzahl neuer Erkenntnisse über Gewebeeigenschaften.

Introduction

In a clinical setting, MRI distinguishes itself from other imaging modalities by its superior contrast in soft tissue. However, some areas appear dark, like lung, bone, ligament, or tendon (▶ **Table 1** for examples), mainly due to the rapid transverse relaxation of the magnetization as typically found in solid tissue with large amounts of bound water or in highly inhomogeneous regions where multiple air-tissue interfaces cause susceptibility variations. The rapid signal decay caused by fast relaxation makes quantitative imaging of such structures challenging, since conventional MRI techniques are unable to capture the signal in time.

Due to the latest developments in hardware, a novel MRI acquisition strategy has gained interest for acquiring information in just such regions. The availability of super-fast switching RF transmitters and receiver coils as well as advanced gradient coils enabled the implementation of sequences with ultrashort echo times (UTE) or even zero echo time (ZTE). Thus, imaging of tissues and components, which were formerly inaccessible to MRI, becomes feasible. In contrast to conventional MRI acquisition strategies, sequences with extremely short echo times can detect a signal from tissues with very short effective transverse relaxation times ($T2^*$). They also allow imaging in areas near magnetic field inhomogeneities or distortions, e. g., near metallic implants, or with multiple susceptibility interfaces, e. g., in lung parenchyma.

A major advantage of UTE and ZTE MR imaging in contrast to CT or other radiographic imaging techniques is the lack of ionizing radiation, which poses a certain, albeit low, risk due to the stochastic nature of ionizing radiation damage. That makes these methods especially attractive for examinations of pediatric patients as well as longitudinal monitoring of disease progression and treatment, where repeated scans would accumulate a high life dose of ionizing radiation [1–6]. For lung imaging it is even estimated that up to 90 % of lung CT examinations could be replaced by ionizing-radiation-free MRI without compromising diagnostic quality [7].

As UTE imaging becomes more widely available, it is broadly investigated in research and will find its place in the clinical routine. Dedicated reviews extensively examine the use of UTE in specific areas in detail, e. g. in musculoskeletal [8, 9], bone [10, 11], or lung MRI [1, 12, 13]. In contrast to these and other comprehensive reviews [14] on technical aspects and numerous possible applications, this study briefly summarizes the major techniques and fields of application. The focus is on routines that are already part of the clinical routine at a limited number of sites and have an impact on patients.

Technical overview

To enable imaging of tissues with ultrafast relaxation times (especially $T2^*$), the echo time (TE), i. e., the time between excitation and readout, must be as short as possible. While conventional MR sequences feature TEs of a few milliseconds, ultrashort or zero echo time sequences can achieve values below 0.2 ms. Both UTE and ZTE are necessarily implemented as gradient echo sequences and therefore are sensitive not only to relaxation due to molecular interactions but also due to magnetic field inhomogeneities. Therefore, an effective transverse magnetization relaxation time (commonly known as $T2^*$), usually much shorter than intrinsic T2, needs to be considered. In a classic MRI sequence with Cartesian k-space sampling, the TE is determined by multiple imaging gradient events required for slice selection and spatial encoding (▶ **Fig. 1A**). The minimal achievable TEs are therefore restricted by hardware performance, especially maximum gradient strength and slew rate, as well as by safety restrictions preventing peripheral nerve stimulation. Current state-of-the-art clinical MRI scanners typically provide gradient strengths of about 45–80 T/m and slew rates of about 200–220 T/m/s [15–17]. Specialized coils can push the slew rate for certain applications up to 500 T/m/s [17].

To avoid time-consuming gradient switching, UTE sequences exploit the possibilities of non-Cartesian k-space sampling, like
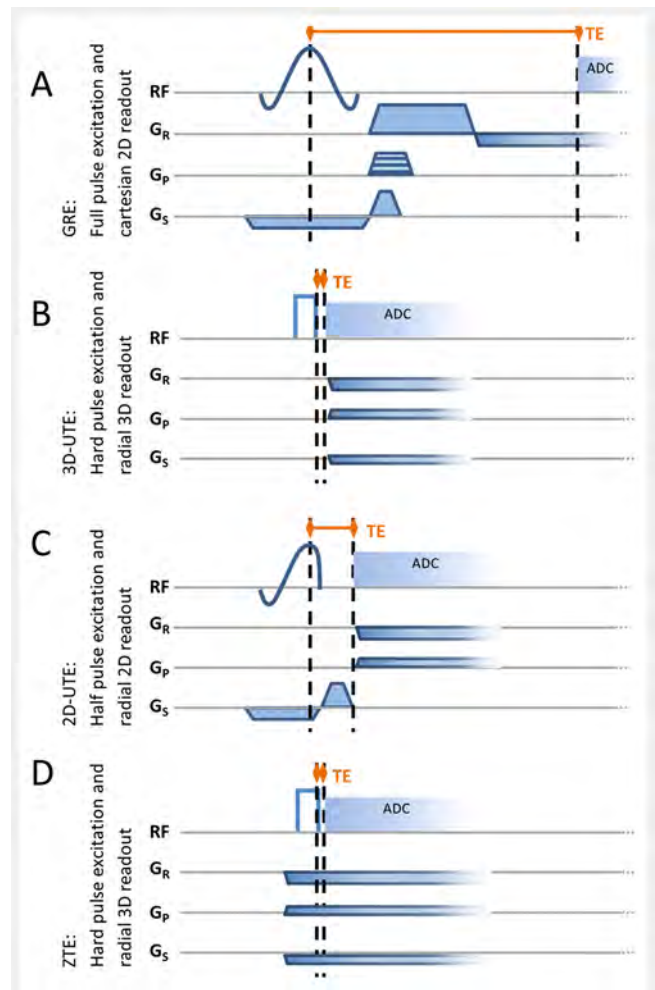
▶ **Table 1** Examples of T2* times in different tissues with ultrashort relaxation times or tissue with ultrafast relaxing components.

Tissue	Long T2* component	Short T2* component	
Osteochondral junction			
▪ Bone	2–3 ms	< 0.5 ms	[15, 22, 55, 63]
▪ Subchondral bone		< 1 ms	[22, 64]
▪ Cartilage	35 ms	0.5 ms	[15]
▪ Knee meniscus	19 ms	2 ms	[15]
▪ Tendon	8–20 ms	< 1 ms	[15]
Skull		1–3 ms	[33]
Lung		0.5–0.85 ms	[4, 39, 65]
White matter		0.42 ms	[48]
▪ Myelin		< 0.3 ms	[16]
▪ Axonal water		33–37 ms	
Carotid plaque calcification		0.31 to 3.87 ms	[55]
Bound water (tendon/collagen)		< 1 ms	[26]
Free water		> 7 ms	[26]

▶ **Fig. 1** Overview of different pulse sequence implementations to achieve ultrashort echo times. **A** standard gradient echo sequence with full pulse and cartesian readout of k-space feature TE times of a few milliseconds. **B** For 3 D acquisitions, no slice encoding gradients are necessary and fast hard pulses can be employed to achieve TE values below 0.2 ms. **C** For 2 D acquisition, TE can be significantly shortened by employing half pulse excitation with VERSE modulation and non-cartesian read-out trajectories, like center-out radial trajectories. **D** In ZTE imaging the read-out gradients are directly started before the excitation pulse. Consequently, the echo time equals the dead time required by the RF amplifiers to switch from excitation to acquisition, which typically lies in the range of 0.04–0.1 ms.

center-out radial or spiral read-out trajectories. By starting each encoding line in the center of k-space, valuable time for phase encoding is saved and sampling is started directly while gradients are still ramping up. Furthermore, most UTE techniques use 3 D k-space sampling with short hard pulses (▶ **Fig. 1B**). For 2D-setups half pulses were suggested in order to shorten the time after the main peak of the excitation pulse [18]. More sophisticated setups, like VERSE pulses [19], will make it possible to further shorten slice selection and associated rephasing gradients (▶ **Fig. 1C**).

Most ZTE sequences pursue a different strategy, where read-out gradients are already starting before the actual excitation pulse in order to save ramp-up times after the pulse (▶ **Fig. 1D**). The main drawback is an acquisition gap thus created in the center of k-space. Several strategies were suggested to acquire the missing data [20]. Promising results for application have been reported for algebraic reconstruction [21], water- and fat-suppressed proton projection MRI (WASPI), which combines a ZTE acquisition with short radial projections [22] or pointwise encoding time reduction with radial acquisition (PETRA), which employs Cartesian single point acquisition to cover the missing central positions in k-space [23, 24].

What remains as the minimum TE in all cases is a technical dead time required to switch the RF amplifiers between excitation and acquisition modes, which typically lies between 0.04–0.1 ms [23, 25] for clinical scanners, but has also been reported to be as low as 0.008 ms [26] or even 0.005 ms employing advanced RF instrumentation hardware [25].

In general, UTE sequences profit from the advantages of non-Cartesian sampling, like robustness to motion. ZTE sequences have the additional advantage of being very quiet as gradients are switched only in small increments. Limitations include the fact that a majority of UTE sequences are 3 D acquisitions, which might be inconvenient for some applications. Moreover, an acquisition that is performed during the gradient ramp-up phase can result in distortions and require correction measures. The

non-uniform sampling of non-Cartesian trajectories is also less efficient than Cartesian sampling schemes and can result in prolonged measurement times. Sophisticated setup of the measurement and trajectory design, e. g. density-corrected k-space sampling methods [27, 28], can mitigate this effect and again drastically shorten measurement time for clinical application.

While similar in their goal, UTE and ZTE sequences pose different challenges to the scanner hardware. While they can in general be implemented on any clinical scanner, the performance and minimum achievable echo times depend on the hardware specifications. UTE sequences profit from high field strengths, for improved SNR, and high gradient amplitude, slew rate, and fidelity to ensure good image quality and resolution. ZTE on the other hand requires no fast gradient switching but continuously high amplitudes and therefore a virtually unlimited duty cycle. Additionally, it demands high standards in terms of RF power transmission and efficiency, which, in contrast, are not crucial for UTE sequences. Both methods profit from rapid switching processes between transmit and receive modes. [29]

UTE images are inherently weighted by proton density and thus offer weak tissue contrast. Therefore, several approaches are described to accentuate fast relaxing tissue compartments [14], including difference imaging and/or magnetization preparation with inversion pulses (▶ **Fig. 2**). The former implies the subtraction of images acquired with ultrashort and moderate TEs (▶ **Fig. 2A**) in order to suppress the signal from slowly relaxing tissue, e. g., from muscles (▶ **Fig. 2B**), bone pores, myocardium, or edemas in musculoskeletal and cardiac imaging. The latter employs preparation pulses to null the signals from non-relevant tissues at the time of acquisition (▶ **Fig. 2D**), like subcutaneous and bone marrow fat in bone imaging or slowly relaxing components in white matter (▶ **Fig. 2E**). A combination of both can further serve to suppress the signal from multiple components posing different relaxation times, e. g. the slowly relaxing components in white and grey matter to enhance the signal from ultrafast relaxing myelin (▶ **Fig. 2G**). Both techniques rely on the assumption of well distinguished compartments with homogeneous relaxation parameters, which might fail in pathological conditions [30, 31]. More advanced techniques, such as the sliding window technique or complex echo subtraction can help to reduce contamination by interfering tissue compartments [9, 14, 32–35].

In addition to structural imaging, quantitative UTE is also of clinical interest to investigate the composition of tissues. Biological tissue is typically composed of several compartments, which are characterized by individual relaxation properties (▶ **Table 1**). The signal of tightly bound water molecules, e. g., in collagen or myelin, decays significantly faster than the signal from less tightly bound or free water molecules, e. g., extracellular water or axonal water. The concentration of short $T2^*$ components may increase in certain pathologies (like fibrosis, iron-deposition, in some stages of hemorrhage and calcification or in deposition diseases or cellular infiltrations) or decrease in others (e. g., edema, infiltration, tumors) [36]. More advanced composition evaluation is achieved by accessing quantitative parameters like $T2^*$ and T1 relaxation times or magnetization transfer properties in dense tissues. UTE is highly relevant for obtaining such quantitative

information, e. g., for $T2^*$ mapping from multi-echo acquisitions (▶ **Fig. 2A, C**), which was previously impossible due to no signal being detectable in ultrafast relaxing tissues.

Joints

Pathological and subclinical changes in joint tissues like tendons, ligaments, and cartilage are one of the most promising applications of UTE imaging [37, 38]. While the low contrast in initial UTE images is not necessarily beneficial in joint imaging, the possibility to gain quantitative values provides significant new information. Next to $T2^*$ mapping, a multi-compartment analysis is of interest to quantify tissue composition and the respective $T2^*$ values of various compartments, which might be derived, e. g. by means of multi-exponential fitting of UTE multi-echo series.

Several studies applied UTE to examine the recovery of tendons after injury or healing progress after reparative surgery [39]. Furthermore, inflammation processes were described as being associated with $T2^*$ changes, reflecting increased extracellular water content and reduced collagen content in tendinopathy [40]. In cartilage, $T2^*$ serves as a biomarker for degenerative processes, e. g. in osteoarthritis [41].

In the Achilles tendon, the short $T2^*$ component was identified as a potential biomarker not only for ageing-related degenerative processes but also for tendinopathy with a specificity of 1 and a sensitivity of 0.86 [42]. In the same study, the reduced amount of bound water in tendinopathy patients was detected with a specificity of 0.43 and a sensitivity of 0.95.

In the shoulder tendons, a recent longitudinal study demonstrated a correlation between the UTE-based $T2^*$ values and the healing process 3, 6, 12, and 24 months after arthroscopic rotator cuff repair surgery, which was evaluated by means of Sugaya classification and patient satisfactory groups [39].

The $T2^*$ relaxation time has also been demonstrated to reflect the impaired integrity of deep cartilage layers, for example after a complex knee trauma. This was demonstrated for example, by an increase in $T2^*$ values of up to 28 % in the cartilage layer of the medial femoral condyle two years after anterior cruciate ligament (ACL) reconstruction [43]. Another clinical study reported an even stronger $T2^*$ increase in the same cartilage region in patients with acute ACL injury and comparable results two years after ACL reconstruction [41].

$T2^*$ relaxation time is also used to characterize meniscal injuries. A study of three cohorts showed that, compared to healthy subjects, $T2^*$ increases in the meniscus up to 27 % in patients with ACL injuries and even more than 90 % in ACL trauma patients with additional, morphologically detectable meniscus injuries [41]. The same study also showed a significant recovery of initial $T2^*$ differences between examined groups two years after ACL reconstruction.

Bone

Bone, as a very dense tissue, has very fast $T2^*$ relaxation times and appears as voids on conventional MRI. At the same time, it fea-
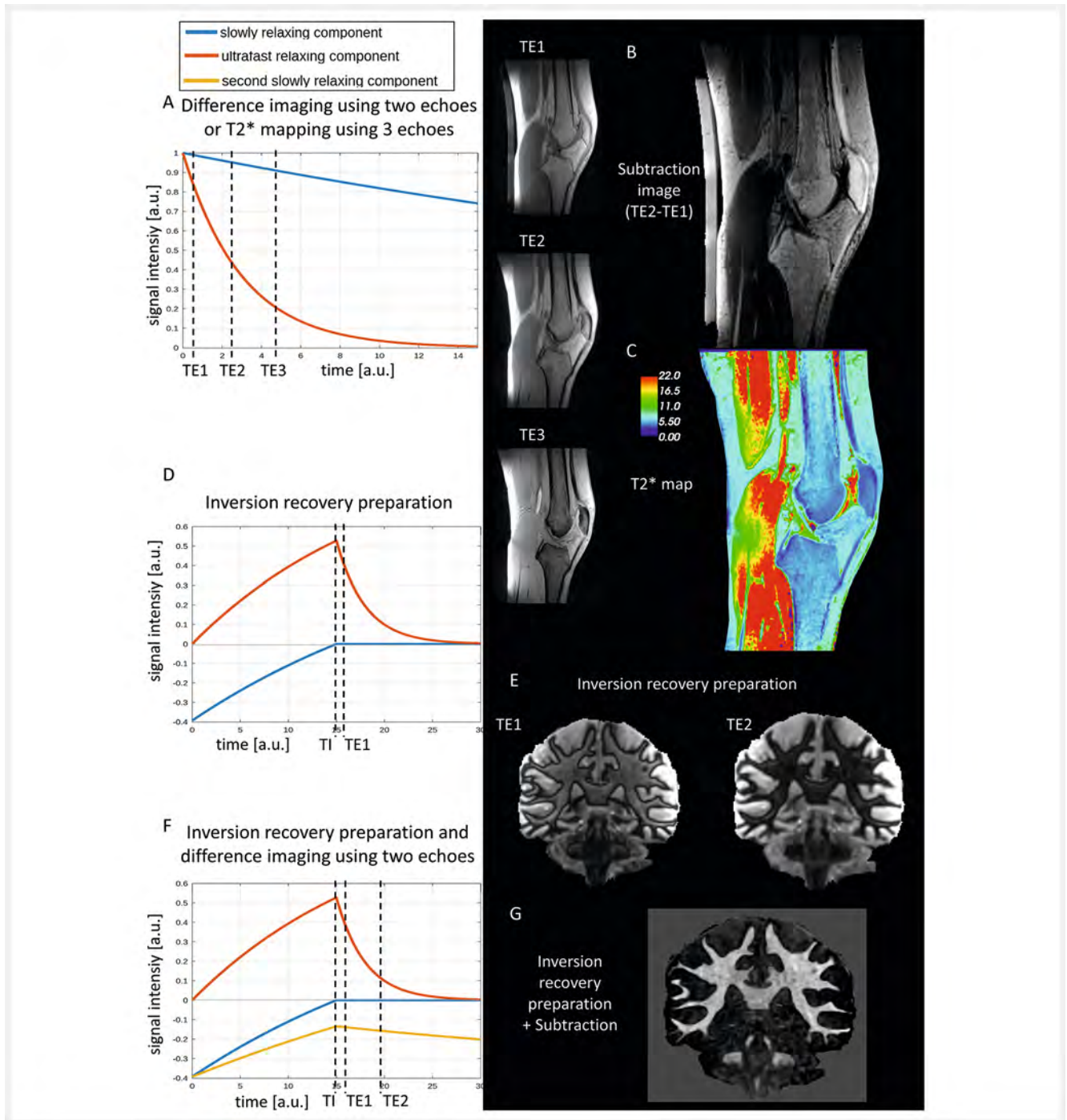
▶ **Fig. 2** To generate contrast for ultrafast relaxing structures in tissues with multiple components, UTE imaging is combined with magnetization preparation and/or difference imaging of two acquisitions with different echo times. **A** T2* relaxation of two components with short (red) and long (blue) relaxation times. By subtracting two images acquired at different echo times (TE1 and TE2), signal from slowly relaxing components can be suppressed. By acquiring multiple echoes (e. g., TE1 to TE6), a (multi-)exponential fit can be performed to quantify T2*-relaxation times. **B** In the knee, an acquisition at two different echo times and subsequent subtraction make it possible to scale down the signal in muscle and fat tissue and enhance the signal from tendons or ligaments. **C** T2* map of the knee calculated from acquisitions at 3 different echo times. **D** An inversion preparation can be employed to suppress the signal of tissues with long T1 relaxation times by setting an appropriate inversion time (TI). Thus, only the signal from fast relaxing structures remains at echo time (TE1). **E** Inversion prepared UTE acquisition in the brain (coronal view) with an inversion time (TI) of 500 ms suppresses the signal of the slowly relaxing components in white matter. The first echo (TE1 = 0.03 ms) shows the considerable signal of fast-relaxing white matter components, whereas the white matter signal is nearly vanished in the second echo (TE2 = 2.5 ms). **F** Combining the inversion preparation and difference imaging makes it possible to suppress the signal from two different slowly relaxing components. **G** In the brain (coronal view), subtraction of two inversion prepared acquisitions at ultrashort and moderate echo times suppresses the signal not only from slowly relaxing components in white matter but also in gray matter, substantially enhancing the contrast of myelin's fast-relaxing components.
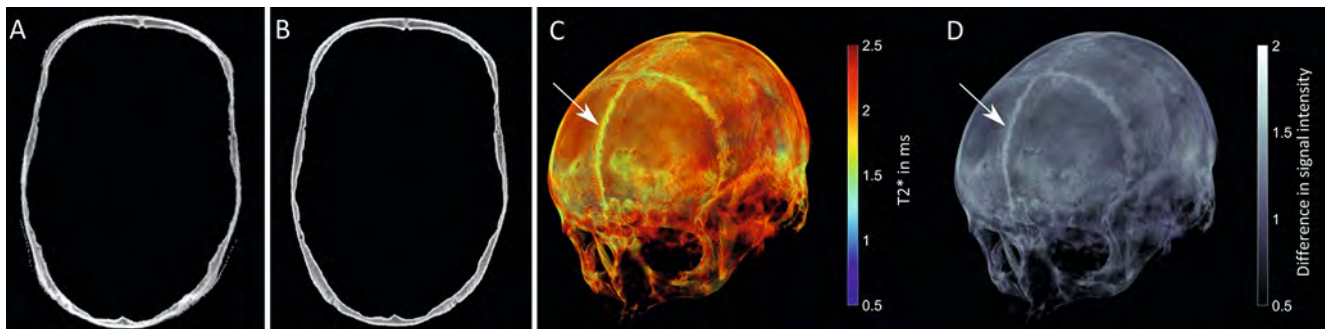
▶ **Fig. 3** Example of morphological and quantitative UTE imaging of cranial bones. Skull, segmented from UTE (**A**) and CT (**B**) acquisition, and 3 D rendering of whole skull of an adult subject with remaining frontal suture (sutura frontalis persistens, indicated by white arrows) segmented from T2* map (**C**) and difference image (**D**) of double echo UTE acquisition, respectively.

tures a complex architecture with multiple compartments that contribute to the UTE signal [9]. Therefore, common UTE techniques in bone imaging include subtraction or double inversion preparation approaches for morphological, CT-like evaluation of injuries, as well as assessment of quantitative markers, which can be used to characterize the bone microstructure and mechanical bone properties like stiffness and elasticity. The latter varies, e. g. depending on age or as a consequence of degenerative structural changes like osteoporosis, and thus determines the risk of bone fractures [11].

The evaluation of the multi-compartment UTE signal decay further allows a selective quantification of free and bound water fractions and thus provides information about the status of bone matrix thinning, as is characteristic in osteoporosis [44]. One highly relevant parameter is the so-called porosity index, defined as a ratio between the signal intensities in bones at moderate and ultra-short TEs, which was previously shown to correlate with porosity metrics in µCT as well as bone stiffness [45]. Furthermore, the macromolecular proton fraction, as it can be assessed by magnetization transfer prepared UTE imaging, uniquely provides information about the amount of bone collagen, and thus allows characterization of the elasticity of bone [46]. Against this background, UTE is a very promising tool for bone status assessment and prediction of fracture risks, e. g., in aging patients or osteoporosis. This is particularly relevant given the moderate sensitivity of conventional diagnosis tools like quantitative CT or dual-energy X-ray absorptiometry (DEXA)-based measurements of mineral bone density [47].

UTE techniques have also been successfully applied to image cranial bone, achieving CT-like contrast of diagnostic quality (▶ **Fig. 3**). Although the spatial resolution obtained by UTE imaging is typically not as high as with CT, overall agreement in visible structural features (e. g., sutura lambdoidea and cranial layers) has been found in both modalities [48]. Consequently, UTE imaging is capable of imaging skull fractures and, when combined with conventional MRI, it is superior to CT for fracture characterization [49]. In addition, the spatial mapping of T2* provides information on cranial bone sublayers and further might enable assessment of post-fracture bone recovery or adolescence development (▶ **Fig. 3C, D**).
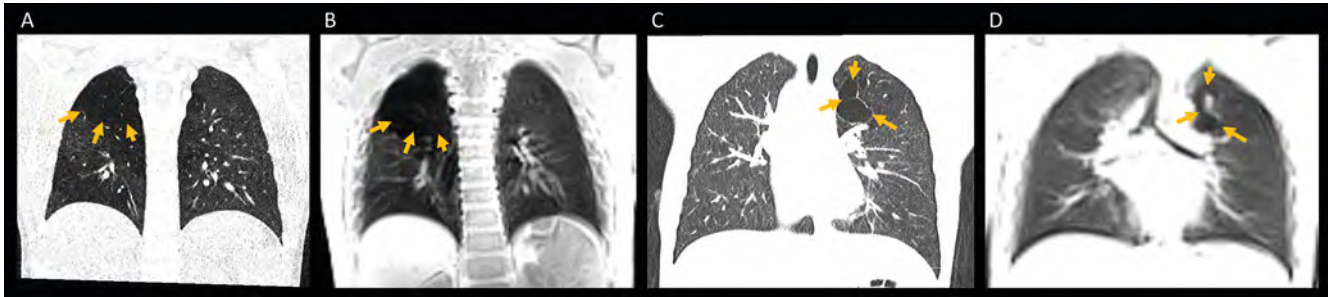
Lung

For a long time, MRI of lung pathologies was of no clinical interest as low proton density and very short T2* times made it almost impossible to gather any signal from the lung parenchyma. This is changing rapidly due, at least in part, to the ongoing introduction of UTE sequences, and research has demonstrated the feasibility of UTE MRI for detecting various lung pathologies. Morphological depiction of the lung parenchyma using UTE imaging can identify hyper- and hypointense areas, which indicate "plus" and "minus" pathologies, respectively. The unique strength of UTE sequences, compared to other MRI sequences, lies in the detection of "minus" pathologies, such as emphysema, congenital lobar overinflation, congenital pulmonary airway malformation, and air trapping (examples shown in ▶ **Fig. 4**). While other MRI sequences are well suited for imaging "plus" pathologies (e. g., atelectasis, inflammatory consolidation, and pulmonary hamartoma) especially with increased water content (like edema, pneumonia, effusion, mucus), UTE imaging also provides adequate visualization in such cases [5, 13].

Current clinical indications for lung MRI include evaluation of cystic fibrosis, lung cancer, and lung nodule characterization as well as pulmonary hypertension [2]. Other pathologies, like pulmonary embolism, pulmonary parenchymal abnormalities, chronic obstructive pulmonary disease, asthma, interstitial lung disease, neonatal lung disease, or obstructive airway diseases are likely to be added to the list shortly [2, 12].

The feasibility of UTE MRI for monitoring cystic fibrosis has been shown and validated against CT and pulmonary function testing for assessing the severity of structural alterations [50]. The functional information obtained thereby can also serve for quantitative analysis of ventilation and hyperinflation [51], characterization of various forms of inflammation, and the detection of small changes in cases of mild cystic fibrosis [52].

Pulmonary thin-section MRI with a UTE sequence can successfully detect lung nodules and can be used to distinguish nodule types [53]. A high sensitivity was shown, especially for the detection of small pulmonary nodules in a range of 4–8 mm [54]. UTE MRI was also employed in a lung cancer screening study and performed comparable to standard- or low-dose CT [55].

▶ **Fig. 4** Images of pediatric patients with air-trapping (**A**, **B**) and congenital pulmonary airway malformation (**C**, **D**) demonstrate the application of UTE for lung imaging of "'minus" pathologies. **A** CT image and **B** UTE image of a case of air-trapping in the upper right lobe, a classic "'minus" pathology, distinguished by a decrease in signal intensity (indicated by yellow arrows). **C** CT imaging of a cyst associated with congenital pulmonary airway malformation, and **D** corresponding UTE image. Arrows indicate the area of reduced signal intensity in the cyst. In contrast to conventional MRI sequences, UTE makes it possible to distinguish such signal losses as it can gain a signal from the surrounding lung parenchyma and therefore provide contrast between healthy tissue and the pathology.

Most recently, chest imaging was considered a vital instrument for the screening, diagnosis, and surveillance of patients during the COVID-19 pandemic [56]. While radiography and CT were employed, concerns about the repeated exposure to ionizing radiation also suggested the use of UTE MR imaging. In fact, UTE MRI was found to be a valuable tool and potential alternative to CT in acute disease as well as post-COVID patients [57, 58].

Brain

Both grey and white matter consist of multiple components with short or long $T2^*$ relaxation times. Initial evaluations of short $T2^*$ components revealed signal variation in multiple pathologies, some of which were not as obvious on conventional MRI, e. g. melanoma metastases, meningeal disease, chronic hepatic encephalopathy, probable calcification, and probable radiation damage [59].

Today, the major focus of UTE in the brain is to directly capture the myelination. As protons in myelin have extremely short $T2^*$ relaxation times of <1 ms, UTE is required for direct assessment [60]. A common approach for selective imaging of protons in myelin is the combination of inversion preparation and difference imaging (▶ **Fig. 2F, G**). By selecting appropriate inversion times (400–500 ms), long $T2^*$ white matter components featuring also long T1 times will be nulled [14, 61, 62]. In addition, the "difference imaging" approach can suppress residual grey matter contributions, which manage to recover through the long inversion process in the preparation phase.

Direct assessment of myelin integrity is of importance for diagnosis, treatment monitoring, and prognosis assessment in many neurological diseases, such as multiple sclerosis (MS), Alzheimer's disease, Parkinson's disease, epilepsy, and traumatic brain injury [14].

In initial exploratory studies in MS patients, inversion pulse prepared UTE imaging revealed differences between lesions and normal-appearing white matter as well as myelin loss in normal-appearing white matter, which was not apparent on T2-FLAIR imaging [63, 64]. Studying the clinical manifestation of MS, a significant correlation was found between direct UTE imaging of myelin and disability in patients [65].

Cardiovascular System

The presence of fast relaxing structures in the cardiovascular system is usually associated with pathological processes, e. g., carotid plaque calcifications or fibrosis. Inversion pulse prepared UTE imaging allows the direct assessment of calcified tissue [66–69]. The assessment of calcifications of coronary arteries, for instance, serves as an independent risk factor for future coronary events [70]. Imaging of calcifications in the carotid artery is another use case as the presence of calcifications may affect the biomechanical stability of atherosclerotic plaques. Because of the high correlation between inversion pulse prepared UTE and CT images of plaque calcifications and the high variability of these plaques [68], UTE-based measurements could therefore serve as an additional tool for MRI-based management of atherosclerosis and plaque classification [69].

Due to its unique capability to detect the collagen signal, UTE imaging is also used to differentiate fibrosis from inflammation, which enhances its utility in cardiac imaging [71]. Visualization of scars in the myocardium, without the need for contrast administration, is a very attractive application of UTE and also opens the door for serial imaging [71].

Apart from tissue characterization, UTE approaches are beneficial for characterizing complicated flow patterns of the cardiovascular system. It has been proven advantageous over conventional MRI sequences in imaging complex flow [72, 73], clipped cerebral aneurysms, and coil embolization [74, 75]. However, UTE-based angiography approaches are still subject to methodological research only.

Methodological Challenges

Despite providing morphological and quantitative information in dense tissues, the UTE techniques are still less common in clinical protocols due to certain limitations. For example, morphologic UTE imaging with high spatial resolution typically requires 3 D

▶ **Table 2** Summary or major fields of application of UTE imaging, main techniques applied in each field, and pathologies in the current focus of UTE imaging.

Area	Main techniques applied	Focus of application	References
Joints	T2* mapping, multi-compartment analysis	Recovery of injured tendons	[39]
		Tendinopathy	[40]
		Osteoarthritis	[41]
Bone	Subtraction or double inversion preparation, quantitative markers	Morphological imaging	[44, 45]
		Fracture risk assessment	[40, 42, 43]
		Osteoporosis and porosity evaluation	[41]
Lung	Short TE imaging	Imaging of minus pathologies	
		Cystic fibrosis,	[50–52]
		Lung cancer and lung nodule characterization	[53–55]
		Pulmonary hypertension	[2]
		Post-COVID	[57, 58]
Brain	Combination of inversion preparation and difference imaging	Myelination	
		Multiple Sclerosis (MS),	[62, 65]
		Neurological diseases	[14]
		Traumatic brain injury	[14]
CV system	Inversion preparation	Atherosclerosis and plaque classification	[68, 69]
		Fibrosis	[71]
		Visualization of scars	[71]
		Characterization of flow	[72, 73]

spatial encoding with a large number of k-space readouts, which is associated with examination times of several minutes. This becomes especially crucial in less compliant patients or in moving organs, e. g., in the heart. In addition, multi-echo-series acquisition for difference imaging or T2* mapping, as well as additional magnetization preparation, required for example to null the interfering tissue compartments or to access the magnetization transfer mechanisms, also extend the examination time. Therefore, slice and in-plane resolutions should be accurately adjusted to the target structures. Furthermore, a moderate signal-to-noise ratio due to low proton density and rapid signal decays in dense tissues makes UTE more susceptible to imaging uncertainties and artifacts. Against this background, more advanced reconstruction and post-processing methods, which employ, for example, compressed sensing or artificial intelligence based approaches, become relevant to face the challenges of UTE imaging with appropriate quality and within a clinically suitable examination time. Finally, non-cartesian k-space sampling often leads to less predictable, radially or spirally shaped interferences between tissues with different chemical shifts, e. g., between fat and water, which might also hamper morphological differentiation. Therefore, appropriate adjustment of readout bandwidth and previously mentioned nulling techniques become important to reduce these artifacts.

Conclusion

In conclusion, ultrashort echo time imaging provides an interesting and very valuable tool for various clinical purposes and promises new insights into tissue properties. UTE (and ZTE) sequences provide a new contrast and capture signal in tissue components formerly invisible on MR imaging due to their very short relaxation times. Besides advanced morphological visualization, quantitative UTE techniques assess relaxation or magnetization transfer properties in ultrafast relaxing structures. Consequently, UTE has found its place in structural lung imaging as well as the characterization of tissue composition and its alterations in musculoskeletal, cardiovascular, or neurodegenerative diseases (▶ **Table 2**). Due to the lack of ionizing radiation exposure, it is especially attractive for pediatric patients and longitudinal monitoring of disease progress and treatment.

Further prospects includes the extension of UTE applications to other pathologies in already mentioned organ systems (e. g., pathologies of central nervous, cardiovascular, musculoskeletal and pulmonary systems) as well as other clinical fields like dentistry or radiation therapy. Furthermore, the clinical potential of UTE imaging can be further elevated by the assessment of additional quantitative parameters like magnetic susceptibility of fast relaxing tissues or by imaging of other nuclei with intrinsically shorter relaxation times, like sodium or phosphorus, which are currently scientific targets only.

Conflict of Interest

The authors declare that they have no conflict of interest.

References

[1] Geiger J, Zeimpekis KG, Jung A et al. Clinical application of ultrashort echo-time MRI for lung pathologies in children. Clin Radiol 2021; 76: 708.e9–708.e17. doi:10.1016/j.crad.2021.05.015

[2] Hatabu H, Ohno Y, Gefter WB et al. Expanding Applications of Pulmonary MRI in the Clinical Evaluation of Lung Disorders: Fleischner Society Position Paper. Radiology 2020; 297: 286–301. doi:10.1148/radiol.2020201138

[3] Renz DM, Herrmann K-H, Kraemer M et al. Ultrashort echo time MRI of the lung in children and adolescents: comparison with non-enhanced computed tomography and standard post-contrast T1w MRI sequences. Eur Radiol 2022; 32: 1833–1842. doi:10.1007/s00330-021-08236-7

[4] Torres L, Kammerman J, Hahn AD et al. "Structure-Function Imaging of Lung Disease Using Ultrashort Echo Time MRI". Acad Radiol 2019; 26: 431–441. doi:10.1016/j.acra.2018.12.007

[5] Veldhoen S, Heidenreich JF, Metz C et al. Three-dimensional Ultrashort Echotime Magnetic Resonance Imaging for Combined Morphologic and Ventilation Imaging in Pediatric Patients With Pulmonary Disease. J Thorac Imaging 2021; 36: 43–51. doi:10.1097/RTI.0000000000000537

[6] Serai SD, Laor T, Dwek JR et al. Feasibility of ultrashort TE (UTE) imaging of children at 1.5 T. Pediatr Radiol 2014; 44: 103–108. doi:10.1007/s00247-013-2758-2

[7] Hirsch FW, Sorge I, Vogel-Claussen J et al. The current status and further prospects for lung magnetic resonance imaging in pediatric radiology. Pediatr Radiol 2020; 50: 734–749. doi:10.1007/s00247-019-04594-z

[8] Afsahi AM, Ma Y, Jang H et al. Ultrashort Echo Time Magnetic Resonance Imaging Techniques: Met and Unmet Needs in Musculoskeletal Imaging. J Magn Reson Imaging JMRI 2022; 55: 1597–1612. doi:10.1002/jmri.28032

[9] Chang EY, Du J, Chung CB. UTE imaging in the musculoskeletal system. J Magn Reson Imaging 2015; 41: 870–883. doi:10.1002/jmri.24713

[10] Du J, Hermida JC, Diaz E et al. Assessment of cortical bone with clinical and ultrashort echo time sequences. Magn Reson Med 2013; 70: 697–704. doi:10.1002/mrm.24497

[11] Ma Y-J, Jerban S, Jang H et al. Quantitative Ultrashort Echo Time (UTE) Magnetic Resonance Imaging of Bone: An Update. Front Endocrinol 2020: 11. doi:10.3389/fendo.2020.567417

[12] Wielpütz MO, Triphan SMF, Ohno Y et al. Outracing Lung Signal Decay – Potential of Ultrashort Echo Time MRI. Fortschr Röntgenstr 2019; 191: 415–423. doi:10.1055/a-0715-2246

[13] Voskrebenzev A, Vogel-Claussen J. Proton MRI of the Lung: How to Tame Scarce Protons and Fast Signal Decay. J Magn Reson Imaging 2021; 53: 1344–1357. doi:10.1002/jmri.27122

[14] Ma Y, Jang H, Jerban S et al. Making the invisible visible-ultrashort echo time magnetic resonance imaging: Technical developments and applications. Appl Phys Rev 2022; 9: 041303. doi:10.1063/5.0086459

[15] Siemens Healthineers. Siemens Healthineers präsentiert zwei revolutionäre High-End-MRTs für Forschung und klinische Routine. Siemens Heal Shape 23 Press. Im Internet: Accessed July 26, 2023 at: https://www.siemens-healthineers.com/deu/press/releases/cimaterrax

[16] Hoogenraad F, Geerts-Ossevoort L, Harvey P. white-paper-ingenia-elition-vega-hp-gradients.pdf. Philips. Im Internet: Accessed July 26, 2023 at: https://www.philips.com/c-dam/b2bhc/us/education/landing-pae/live-webinar-optimizing-mr-workflow/white-paper-ingenia-elition-vega-hp-gradients.pdf

[17] Kelley D. Development of high-performance gradient systems. GE Healthc SIGNA™ Pulse MR. Im Internet: Accessed July 26, 2023 at: https://signapulse.gehealthcare.com/development-of-high-performance-gradient-sys-aea2l

[18] Pauly JM, Conolly SM, Nishimura DG et al. Slice-selective excitation for very short T2 species. In: Proceedings of the SMRM 8th Annual Meeting. 28 Amsterdam, The Netherlands, 1989

[19] Conolly S, Nishimura D, Macovski A et al. Variable-rate selective excitation. J Magn Reson 1969 1988; 78: 440–458. doi:10.1016/0022-2364(88)90131-X

[20] Froidevaux R, Weiger M, Brunner DO et al. Filling the dead-time gap in zero echo time MRI: Principles compared. Magn Reson Med 2018; 79: 2036–2045. doi:10.1002/mrm.26875

[21] Weiger M, Pruessmann KP. MRI with Zero Echo Time. EMagRes Eds RK Harris RL Wasylishen 2012. doi:10.1002/9780470034590.emrstm1292

[22] Wu Y, Dai G, Ackerman JL et al. Water- and fat-suppressed proton projection MRI (WASPI) of rat femur bone. Magn Reson Med 2007; 57: 554–567. doi:10.1002/mrm.21174

[23] Grodzki DM, Jakob PM, Heismann B. Ultrashort echo time imaging using pointwise encoding time reduction with radial acquisition (PETRA). Magn Reson Med 2012; 67: 510–518. doi:10.1002/mrm.23017

[24] Dournes G, Grodzki D, Macey J et al. Quiet Submillimeter MR Imaging of the Lung Is Feasible with a PETRA Sequence at 1.5 T. Radiology 2015; 276: 258–265. doi:10.1148/radiol.15141655

[25] Weiger M, Brunner DO, Dietrich BE et al. ZTE imaging in humans. Magn Reson Med 2013; 70: 328–332. doi:10.1002/mrm.24816

[26] Brittain J, Shankaranarayanan A, Ramana V et al. Ultra-short TE imaging with single-digit (8 μs) TE. In: Proceedings of the 12th Annual Meeting of ISMRM. Kyoto, Japan, 2004

[27] Nielles-Vallespin S, Weber M-A, Bock M et al. 3D radial projection technique with ultrashort echo times for sodium MRI: Clinical applications in human brain and skeletal muscle. Magn Reson Med 2007; 57: 74–81. doi:10.1002/mrm.21104

[28] Johnson KM, Fain SB, Schiebler ML et al. Optimized 3D ultrashort echo time pulmonary MRI. Magn Reson Med 2013; 70: 1241–1250. doi:10.1002/mrm.24570

[29] Weiger M, Pruessmann KP. Short-T2 MRI: Principles and recent advances. Prog Nucl Magn Reson Spectrosc 2019; 114–115: 237–270. doi:10.1016/j.pnmrs.2019.07.001

[30] Whittall KP, Mackay AL, Graeb DA et al. In vivo measurement of T2 distributions and water contents in normal human brain. Magn Reson Med 1997; 37: 34–43. doi:10.1002/mrm.1910370107

[31] Manhard MK, Harkins KD, Gochberg DF et al. 30-Second bound and pore water concentration mapping of cortical bone using 2D UTE with optimized half-pulses. Magn Reson Med 2017; 77: 945–950. doi:10.1002/mrm.26605

[32] Jang H, Carl M, Ma Y et al. Inversion recovery zero echo time (IR-ZTE) imaging for direct myelin detection in human brain: a feasibility study. Quant Imaging Med Surg 2020; 10: 89506–89906. doi:10.21037/qims.2020.04.13

[33] Ma Y-J, Searleman AC, Jang H et al. Whole-Brain Myelin Imaging Using 3D Double-Echo Sliding Inversion Recovery Ultrashort Echo Time (DESIRE UTE) MRI. Radiology 2020; 294: 362–374. doi:10.1148/radiol.2019190911

[34] Manhard MK, Horch RA, Gochberg DF et al. In Vivo Quantitative MR Imaging of Bound and Pore Water in Cortical Bone. Radiology 2015; 277: 221–229. doi:10.1148/radiol.2015140336

[35] Horch RA, Gochberg DF, Nyman JS et al. Clinically compatible MRI strategies for discriminating bound and pore water in cortical bone. Magn Reson Med 2012; 68: 1774–1784. doi:10.1002/mrm.24186

[36] Tyler DJ, Robson MD, Henkelman RM et al. Magnetic resonance imaging with ultrashort TE (UTE) PULSE sequences: Technical considerations. J Magn Reson Imaging 2007; 25: 279–289. doi:10.1002/jmri.20851

[37] Lansdown DA, Ma CB. Clinical Utility of Advanced Imaging of the Knee. J Orthop Res 2020; 38: 473–482. doi:10.1002/jor.24462

[38] Cheng KY, Moazamian D, Ma Y et al. Clinical application of ultrashort echo time (UTE) and zero echo time (ZTE) magnetic resonance (MR) imaging in the evaluation of osteoarthritis. Skeletal Radiol 2023. doi:10.1007/s00256-022-04269-1

[39] Xie Y, Liu S, Qu J et al. Quantitative Magnetic Resonance Imaging UTE-T2* Mapping of Tendon Healing After Arthroscopic Rotator Cuff Repair: A Longitudinal Study. Am J Sports Med 2020; 48: 2677–2685. doi:10.1177/0363546520946772

[40] Xu Y, Murrell GAC. The Basic Science of Tendinopathy. Clin Orthop 2008; 466: 1528–1538. doi:10.1007/s11999-008-0286-4

[41] Chu CR, Williams AA, West RV et al. Quantitative Magnetic Resonance Imaging UTE-T2* Mapping of Cartilage and Meniscus Healing After Anatomic Anterior Cruciate Ligament Reconstruction. Am J Sports Med 2014; 42: 1847–1856. doi:10.1177/0363546514532227

[42] Loegering IF, Denning SC, Johnson KM et al. Ultrashort echo time (UTE) imaging reveals a shift in bound water that is sensitive to sub-clinical tendinopathy in older adults. Skeletal Radiol 2021; 50: 107–113. doi:10.1007/s00256-020-03538-1

[43] Titchenal MR, Williams AA, Chehab EF et al. Cartilage Subsurface Changes to Magnetic Resonance Imaging UTE-T2* 2 Years After Anterior Cruciate Ligament Reconstruction Correlate With Walking Mechanics Associated With Knee Osteoarthritis. Am J Sports Med 2018; 46: 565–572. doi:10.1177/0363546517743969

[44] Xia N, Cai Y, Kan Q et al. The role of microscopic properties on cortical bone strength of femoral neck. BMC Musculoskelet Disord 2023; 24: 133. doi:10.1186/s12891-023-06248-6

[45] Hong AL, Ispiryan M, Padalkar MV et al. MRI-derived bone porosity index correlates to bone composition and mechanical stiffness. Bone Rep 2019; 11: 100213. doi:10.1016/j.bonr.2019.100213

[46] Jerban S, Ma Y, Dorthe EW et al. Assessing cortical bone mechanical properties using collagen proton fraction from ultrashort echo time magnetization transfer (UTE-MT) MRI modeling. Bone Rep 2019; 11: 100220. doi:10.1016/j.bonr.2019.100220

[47] Manhard MK, Nyman JS, Does MD. Advances in imaging approaches to fracture risk evaluation. Transl Res 2017; 181: 1–14. doi:10.1016/j.trsl.2016.09.006

[48] Krämer M, Herzau B, Reichenbach JR. Segmentation and visualization of the human cranial bone by T2* approximation using ultra-short echo time (UTE) magnetic resonance imaging. Z Für Med Phys 2020; 30: 51–59. doi:10.1016/j.zemedi.2019.06.003

[49] Wu H, Zhong Y, Nie Q et al. Feasibility of three-dimensional ultrashort echo time magnetic resonance imaging at 1.5 T for the diagnosis of skull fractures. Eur Radiol 2016; 26: 138–146. doi:10.1007/s00330-015-3804-2

[50] Benlala I, Point S, Leung C et al. Volumetric quantification of lung MR signal intensities using ultrashort TE as an automated score in cystic fibrosis. Eur Radiol 2020; 30: 5479–5488. doi:10.1007/s00330-020-06910-w

[51] Heidenreich JF, Weng AM, Metz C et al. Three-dimensional Ultrashort Echo Time MRI for Functional Lung Imaging in Cystic Fibrosis. Radiology 2020; 296: 191–199. doi:10.1148/radiol.2020192251

[52] Dournes G, Walkup LL, Benlala I et al. The Clinical Use of Lung MRI in Cystic Fibrosis: What, Now, How? Chest 2021; 159: 2205–2217. doi:10.1016/j.chest.2020.12.008

[53] Ohno Y, Koyama H, Yoshikawa T et al. Standard-, Reduced-, and No-Dose Thin-Section Radiologic Examinations: Comparison of Capability for Nodule Detection and Nodule Type Assessment in Patients Suspected of Having Pulmonary Nodules. Radiology 2017; 284: 562–573. doi:10.1148/radiol.2017161037

[54] Burris NS, Johnson KM, Larson PEZ et al. Detection of Small Pulmonary Nodules with Ultrashort Echo Time Sequences in Oncology Patients by Using a PET/MR System. Radiology 2016; 278: 239–246. doi:10.1148/radiol.2015150489

[55] Ohno Y, Takenaka D, Yoshikawa T et al. Efficacy of Ultrashort Echo Time Pulmonary MRI for Lung Nodule Detection and Lung-RADS Classification. Radiology 2022; 302: 697–706. doi:10.1148/radiol.211254

[56] Rubin GD, Ryerson CJ, Haramati LB et al. The Role of Chest Imaging in Patient Management During the COVID-19 Pandemic: A Multinational Consensus Statement From the Fleischner Society. Chest 2020; 158: 106–116. doi:10.1016/j.chest.2020.04.003

[57] Yang S, Zhang Y, Shen J et al. Clinical Potential of UTE-MRI for Assessing COVID-19: Patient- and Lesion-Based Comparative Analysis. J Magn Reson Imaging 2020; 52: 397–406. doi:10.1002/jmri.27208

[58] Fauveau V, Jacobi A, Bernheim A et al. Performance of spiral UTE-MRI of the lung in post-COVID patients. Magn Reson Imaging 2023; 96: 135–143. doi:10.1016/j.mri.2022.12.002

[59] Waldman A, Rees JH, Brock CS et al. MRI of the brain with ultra-short echo-time pulse sequences. Neuroradiology 2003; 45: 887–892. doi:10.1007/s00234-003-1076-z

[60] Lecar H, Ehrenstein G, Stillman I. Detection of Molecular Motion in Lyophilized Myelin by Nuclear Magnetic Resonance. Biophys J 1971; 11: 140–145. doi:10.1016/S0006-3495(71)86203-3

[61] Du J, Ma G, Li S et al. Ultrashort echo time (UTE) magnetic resonance imaging of the short T2 components in white matter of the brain using a clinical 3T scanner. NeuroImage 2014; 87: 32–41. doi:10.1016/j.neuroimage.2013.10.053

[62] Ma Y-J, Jang H, Chang EY et al. Ultrashort echo time (UTE) magnetic resonance imaging of myelin: technical developments and challenges. Quant Imaging Med Surg 2020; 10: 1186–1203. doi:10.21037/qims-20-541

[63] Ma Y-J, Jang H, Wei Z et al. Myelin Imaging in Human Brain Using a Short Repetition Time Adiabatic Inversion Recovery Prepared Ultrashort Echo Time (STAIR-UTE) MRI Sequence in Multiple Sclerosis. Radiology 2020; 297: 392–404. doi:10.1148/radiol.2020200425

[64] Sheth V, Shao H, Chen J et al. Magnetic resonance imaging of myelin using ultrashort Echo time (UTE) pulse sequences: Phantom, specimen, volunteer and multiple sclerosis patient studies. NeuroImage 2016; 136: 37–44. doi:10.1016/j.neuroimage.2016.05.012

[65] Jang H, Ma Y-J, Chang EY et al. Inversion Recovery Ultrashort TE MR Imaging of Myelin is Significantly Correlated with Disability in Patients with Multiple Sclerosis. Am J Neuroradiol 2021; 42: 868–874. doi:10.3174/ajnr.A7006

[66] Chan CF, Keenan NG, Nielles-Vallespin S et al. Ultra-short echo time cardiovascular magnetic resonance of atherosclerotic carotid plaque. J Cardiovasc Magn Reson Off J Soc Cardiovasc Magn Reson 2010; 12: 17. doi:10.1186/1532-429X-12-17

[67] Du J, Corbeil J, Znamirowski R et al. Direct imaging and quantification of carotid plaque calcification: Imaging of CPC. Magn Reson Med 2011; 65: 1013–1020. doi:10.1002/mrm.22682

[68] Du J, Peterson M, Kansal N et al. Mineralization in calcified plaque is like that of cortical bone–further evidence from ultrashort echo time (UTE) magnetic resonance imaging of carotid plaque calcification and cortical bone. Med Phys 2013; 40: 102301. doi:10.1118/1.4819944

[69] Sharma S, Boujraf S, Bornstedt A et al. Quantification of calcifications in endarterectomy samples by means of high-resolution ultra-short echo time imaging. Invest Radiol 2010; 45: 109–113. doi:10.1097/RLI.0-b013e3181c8cefa

[70] Achenbach S, Daniel WG. Current role of cardiac computed tomography. Herz 2007; 32: 97–107. doi:10.1007/s00059-007-2961-8

[71] Schuijf JD, Ambale-Venkatesh B, Kassai Y et al. Cardiovascular ultrashort echo time to map fibrosis-promises and challenges. Br J Radiol 2019; 92: 20190465. doi:10.1259/bjr.20190465

[72] Krämer M, Motaal AG, Herrmann K-H et al. Cardiac 4D phase-contrast CMR at 9.4 T using self-gated ultra-short echo time (UTE) imaging. J Cardiovasc Magn Reson 2017; 19: 39. doi:10.1186/s12968-017-0351-9

[73] Zhang C, Dou W, Yu K et al. The feasibility of non-contrast-enhanced zero echo time magnetic resonance angiography for characterization of intracranial atherosclerotic disease. Quant Imaging Med Surg 2021; 11: 2442–2452. doi:10.21037/qims-20-696

[74] Katsuki M, Narita N, Ozaki D et al. Three tesla magnetic resonance angiography with ultrashort echo time describes the arteries near the cerebral aneurysm with clip and the peripheral cerebral arteries. Surg Neurol Int 2020; 11: 224. doi:10.25259/SNI_329_2020

[75] Takano N, Suzuki M, Irie R et al. Non-Contrast-Enhanced Silent Scan MR Angiography of Intracranial Anterior Circulation Aneurysms Treated with a Low-Profile Visualized Intraluminal Support Device. Am J Neuroradiol 2017; 38: 1610–1616. doi:10.3174/ajnr.A5223